Submitted to Geophysical Journal International, 2002

Epicenter accuracy based on seismic network criteria

István Bondár[1], Stephen C. Myers[2], E. Robert Engdahl[3] and Eric A. Bergman[4]

[1]*Science Applications International Corp., Center for Monitoring Research, ibondar@cmr.gov*

[2]*Lawrence Livermore National Laboratory, smyers@llnl.gov*

[3]*University of Colorado at Boulder, engdahl@colorado.edu*

[4]*Global Seismological Services, bergman@seismo.com*

SUMMARY

A large variety of seismic studies rely on seismic catalog data for event locations and parameters. Event location and uncertainty parameters in most of the global, regional and national earthquake catalogs are obtained from traditional linearized inversion methods using a one-dimensional earth model to predict travel-times. However, assessing location accuracy based on formal uncertainties can be misleading, as those depend on Gaussian, zero mean, uncorrelated error processes. Unfortunately, these assumptions are violated in many catalog locations leading to the underestimation of true location error, especially at high confidence levels. Our objective is to establish reliable, conservative estimates for epicenter location accuracy using data readily available in routinely published catalogs. We assess epicenter accuracy based on station geometry and develop criteria based on primary and secondary azimuthal gaps for local, near-regional and teleseismic networks.

We use confidence levels to describe epicenter accuracy instead of upper bound designations, which are often confounded by outliers. The local network selection criteria are developed from explosions with exactly known epicenters. We also use a well-located (accuracy of 5 km or better) data set of earthquakes and explosions to derive candidate reference event selection criteria for regional and teleseismic networks. We show that earthquakes are less accurately located by regional and teleseismic networks than explosions. In each case we use a Monte Carlo simulation to validate the network criteria

Key words: epicenter accuracy, seismic calibration

1 INTRODUCTION

Although there is a considerable effort to develop non-linear inversion schemes to estimate event locations and the corresponding uncertainties (Rodi et al., 2002, Sambridge and Kennett, 2001) as well as applying three-dimensional Earth models for travel-time predictions (Ritzwoller et al., 2002, Antolik et al., 2001, McLaughlin et al., 2002) these methods and Earth models have yet to find their way to routine production of earthquake catalogs. Currently almost all published earthquake bulletins apply traditional, iterative linearized inversion schemes and one-dimensional earth models to obtain event location and uncertainty parameters. Futhermore, the goal of catalog producers is to achieve completeness to the lowest magnitude, which is at odds with maintaining location accuracy across the catalog. As a result catalogs are "contaminated" with poor

quality locations. Our objective is to establish reliable estimates of epicenter accuracy based on parameters that are readily available in published earthquake catalogs. Using these criteria, high-quality subsets of catalog epicenters can be selected for structural and calibration studies.

Analysis of seismic location accuracy is traditionally based on formal uncertainty. Most location algorithms rely on one of two methods to determine uncertainty. The first is based on the F-statistic, where the *a posteriori* residual distribution is mapped to a location confidence ellipsoid (Flinn, 1965). The second is based on the chi-square statistic, where *a priori* uncertainty for phase picking and travel-time prediction are mapped though the location algorithm to produce a coverage ellipsoid (Evernden, 1969). Proper application of either technique requires compliance with basic statistical assumptions. Both methods require Gaussian, zero mean, uncorrelated error processes. A number of studies suggest that these assumptions are violated in most seismic locations. Picking error tends to have "heavy" tails (Buland, 1986) and may be multimodal. The mean path-specific, travel-time prediction error is typically not zero and travel-time prediction errors are typically correlated for similar ray paths (e.g. Myers and Schultz, 2000a).

Violation of statistical assumptions results in unrepresentative uncertainty analysis, causing underestimation of true error (Myers and Schultz, 2000). Perhaps the most critical, and commonly violated assumption is that travel-time prediction errors are

unbiased. The use of a one-dimensional model to predict travel-times in the three-dimensional earth, results in travel-time bias along specific paths. A classic example of travel-time prediction bias resulting from unmodeled 3-D earth structure is the Long Shot Nuclear explosion (Herrin and Taggart, 1968). In this case, travel paths to many stations sample a subducted oceanic lithosphere with high seismic velocity, causing travel-time prediction errors to be systematically late. Using large numbers of arrivals in the location, which are assumed to be uncorrelated, results in a small formal error ellipse (139 km^2). However, the seismic location error is 26 km, far outside of the confidence ellipse error. A classic example of local network location biases occurs on the San Andreas fault, where seismic velocities are faster on one side of the fault than the other. Dewey and Kork (2000) showed that the location bias is as high as 5 km for events that are well-recorded on a local network in Central California.

Seismic catalogs are used in a wide variety of studies ranging from seismic hazard to the development of earth models. For example, it was recognized early on that accurately located events are needed to develop and test 1D travel-time tables. Herrin (1968) used arrival times from nuclear explosions with exactly known hypocenters and origin times to construct travel-time tables, bypassing the issue of location uncertainty for earthquakes. However, spatial sampling is limited when only explosions are used to construct global models, so Kennett and Engdahl (1991) augmented explosions with well-located earthquakes. Although the goal of using well-located events was to obtain location accuracy of 5 km, this level of accuracy was a best guess.

It is clear that formal uncertainty reported in catalogs cannot be taken at face value and that methods of gleaning location accuracy from the information provided in catalogs is important. Many studies have recognized the need for assessing location accuracy for catalog data, but to date the criteria for selecting events are often vague and the degree of accuracy is an educated guess.

1.1 Review of location accuracy assessment

Assessment of location accuracy has a long history. Most recently, improved location accuracy has been central in efforts to effectively monitor the Comprehensive Nuclear Test Ban Treaty. Much of the recent work is not published in the open literature. Here we review published and unpublished efforts that have contributed to the methods and findings presented below.

Kennett and Engdahl (1991) assessed location accuracy for nuclear explosions and well-located earthquakes using the iasp91 velocity model and found an average error of 14 km. Sweeney (1996) investigated the feasibility of selecting reference events from mostly teleseismic, global bulletins, such as the International Seismological Centre (ISC) and National Earthquake Information Center (NEIC) catalogs. He suggested that events have a location accuracy of 10-15 km when located with an azimuthal gap less than 200° and with at least 50 phases. Sweeney (1998) revisited the selection criteria and found 15 km epicenter accuracy for teleseismic networks with azimuthal gap of 90° and with at least 50 defining phases. Engdahl et al., (1998) produced the EHB catalog by using path-

specific travel-time corrections and a groomed ISC catalog. They assessed the error relative to worldwide nuclear explosion locations and determined a 7 km average mislocation when the azimuthal gap is less than 180°. Myers and Schultz (2000a) found 15 km epicenter accuracy at the 95% confidence level for EHB events with azimuthal gap of less than 90°. A caveat on this validation study is that events near subduction zones, which may be biased by the influence of subducted lithosphere, are not tested. These criteria were used by several studies (Myers and Schultz, 2000b; Steck et al., 2001) for selecting calibration events to develop and validate empirical travel-time correction surfaces. Bondár et al. (2001) introduced various ground truth categories (GTX, where "X" designates epicenter location accuracy in kilometers, that is, the true epicenter lies within "X" km of the estimated epicenter) to describe the location accuracy of events in the CMR Ground Truth database. Events satisfying Sweeney's (1998) criteria were accepted as GT25, while for GT10 at least 5 stations within 2° distance and an azimuthal gap less than 180° for stations within 5° distance were required, basically prescribing a local network solution.

For local and regional catalogs Dewey et al. (1999) established "stringent" and "relaxed" criteria to select events with 10 km accuracy using the NEIC catalogue. Their stringent selection criteria require that events are greater then mb=3.5 and located with 1) at least 10 stations within 250 km from the epicenter, 2) at least one station within 30 km, and 3) an azimuthal gap less than 90°. Their relaxed criteria require a 180° gap with 5 stations within 250 km and at least one station within 30 km. They validated the selection criteria

by locating the events with random sparse subsets of stations and compared the locations to that obtained from using all stations. They note that events meeting either the stringent or the relaxed criteria are only GT10 candidates. To accept an event as GT10, it is required that the relocated events, using only local stations and a local velocity model, be consistent with the regional network location, i.e. be within 5 km from the regional network location and the semi-major axis of the 90% confidence ellipse be less than 5 km. Dewey and Kork (2001) pointed out that some of the events selected by the stringent criteria may be accepted as GT5. To accept an event as GT5 they required that the relocated event be within 2.5 km from the regional network location and the semi-major axis of the 90% confidence ellipse be less than 2.5 km for events not in a source region with known high bias.

McLaughlin et al., (2002) adopted Dewey's stringent criteria in a somewhat relaxed form to select GT5 events. The selection criteria for candidate GT5 events required that shallow-focus events are located with at least 10 stations with an azimuthal gap less than 120° within 250 km from the epicenter and at least one station within 30 km. For utility in regional calibration, it is also required that the event be recorded beyond 250 km. However, Myers and Schultz (2001) pointed out that these GT5 selection criteria are not stringent enough. Using the Dead Sea calibration explosion they selected random subsets of stations that satisfy the constraints of the GT5 selection criteria and relocated the event. The comparison with the GT0 location of the explosion demonstrated that location

accuracy is 12 km at the 95% confidence level and mislocation can be as high as 20 km. In section 4.1. we revisit these criteria.

Multiple event location techniques, such as Hypocentroidal Decomposition (HDC) (Jordan and Sverdrup, 1981; Engdahl and Bergman, 2000, 2001) and Joint Hypocenter Determination (JHD) (Douglas, 1967; Dewey, 1991; Israelsson et al., 2000) have also been used to validate candidate GT5 events. Candidate reference events are validated if multiple event location of clustered events, using phases from regional and teleseismic distance ranges, are consistent with the corresponding local network solutions. Events, not originally identified as GT5 candidates in the clusters, may be promoted to GT5 level if the semi-major axis of their 90% confidence ellipse is less than 5 km.

This study is a new look at the location accuracy criteria. We examine criteria for local, regional, and teleseismic networks, as well as criteria and validation using explosion and earthquake data sets.

2 DATA SETS

2.1 Fiducial explosions

In November of 1999 three calibration explosions were detonated in the Dead Sea (Gitterman and Shapiro, 2001). The yields for these explosions were 0.5, 2 and 5 tons of TNT. The smallest explosion was recorded only on the closest stations, but the two larger events were recorded on stations in Israel, Jordan, Lebanon, and Syria to distances of 250 km. The combined local network provides excellent network coverage with considerable

azimuthal redundancy. Records of the 5-ton explosion are highest in quality and are therefore used in this study. P-wave picks were provided through the Eastern Mediterranean Seismological Center and directly from the Geophysical Institute of Israel. S-wave arrivals for these underwater explosions are not evident in the records.

On 2 November 1992 an accident at an ammunition storage site in the Swiss Alps killed six people and blasted off about 1 million cubic meters of rock. The nominal yield for the explosion is 0.83 kiloton TNT. However, the exact time of the explosion is not known and the best origin time estimation is from the `fixed location' using the stations of the Swiss Seismological Service. Fig. 1 shows the local station distribution for the Dead Sea (Fig. 1a) and the ammunition storage explosion (Fig. 1b).

It should be noted that both GT0 explosions lie in fairly complex regions where 3-D heterogeneities can be expected. To our best knowledge these are the only GT0 events with the requisite station coverage to carry out a Monte Carlo simulation. Because of the complex geology, these events provide conservative estimates of location accuracy, as simpler geologic settings are likely to afford more accurately locations.

On 28 May 1998 Pakistan carried out its first underground nuclear explosion. The event was teleseismically well-recorded and both Albright et al., (1998) and Barker et al., (1998) determined the epicenter under the same mountain using satellite imagery. Since the two epicenters are 4.5 km from each other, we consider the event GT5. Barker et al., (1998) estimated the yield between 6 and 13 kiloton, at the 95% confidence level. This

explosion, in combination with earthquakes located with 5 km accuracy (described below), forms the validation data set for teleseismic networks.

2.2 Well-Constrained Earthquakes and Explosions

We assembled a database of globally distributed seismic events that were well recorded at regional and teleseismic distances and whose absolute locations and origin times are known to higher accuracy than is typical of even the best global earthquake catalog (Fig. 2). The database is used in this study to establish representative criteria for location accuracy over regional and teleseismic distance ranges. Foremost among the sources of data is the CMR Ground Truth and Explosion databases (Bondár et al., 2001; Yang et al., 2000) of contributed source parameters for earthquakes, nuclear explosions and other seismic sources. Engdahl and Bergman (2001) also provided a large number of well-located earthquakes and explosions that have been validated by multiple event location methods. There are currently 1905 events in the database, including 1234 explosions, most with source locations known to 2 km or better, and 671 earthquakes whose locations are believed to be accurate to at least 5 km. For each event, the associated phase arrival times are primarily taken from the ISC catalog. We refer to this data set as GT5 database or data set in the rest of the paper.

Clustered events in the GT5 database are validated by the Hypocentroidal Decomposition (HDC) method (Jordan and Sverdrup, 1981) for multiple event relocation. We seek situations where a number of moderate-size explosions or earthquakes are clustered

(within about 50-100 km of each other) and where the location of at least one of the explosions is known to within at most 2 km or, in the case of earthquakes, has been very well located by a local network. The events in the cluster may be widely distributed in time, as long as arrival time data are available. We validate candidate reference events by requiring that the relative patterns of candidate reference events are consistent with the pattern of the corresponding cluster vectors from the HDC analysis. Discrepancies may be resolved by determining that the cluster vector is biased for some reason, or by rejecting the candidate reference event. For this reason, most of the clusters contributed to the database for this study are calibrated by several reference events.

For this study a modified version of the algorithm developed by Engdahl et al. (1998) was used to perform relocation tests on all events in the GT5 database. This is a single-event location procedure that uses the AK135 travel-time model (Kennett et al., 1995), and features both dynamic phase identification and weights based on the inverse of previously determined phase variances as a function of distance. Outliers are removed dynamically by truncation; 7.5 sec for arrivals up to 28 degrees surface-focus distance and 3.5 sec at larger (teleseismic) distances. For these tests, depths were fixed at the depth of the reference event in all EHB relocations, only first arriving P waves were used as defining phases, and no patch (station) corrections were applied. Ellipticity and elevation corrections were, however, applied to the predicted travel-times. For the relocation tests made in this study, event convergence, (i.e. changes in location and origin

time of less than 0.1 km and 0.01 sec, respectively) was usually achieved after several iterations regardless of the station distribution.

Fig. 3 shows the distributions of first-arriving P-wave travel-time residuals for earthquakes (left) and explosions (right) in near regional, regional and teleseismic distance ranges. The vertical axis indicates the percentage of the observations in a bin relative to the total number of observations. All residuals are from defining phases, with origin times adjusted to fit the AK135 model. We note the striking difference between the travel-time distribution patterns of earthquakes and explosions. The effect of systematic travel-time errors is smeared out by the poorer location accuracy and larger picking errors in the earthquake population. Therefore we treat the earthquake and explosion populations separately and rely on the earthquakes when deriving selection criteria for candidate reference events. We further discuss the discrepancy between the earthquake and explosion population in section 4.1.

3 DISTANCE-DEFINED NETWORK CATEGORIES

In this study we examine location accuracy for local, near-regional, regional, and teleseismic networks separately. The primary utility in segregating locations by network distance is that both travel-time prediction and arrival picking statistics tend to be distinct in each distance range.

We extend common definitions of *local* distance (between 0° and the Pn/Pg crossover) to include arrivals out to 2.5°. Inclusion of data at and slightly beyond the Pn/Pg crossover

distance likely increases location error. Our local distance criteria are, therefore, conservative estimates, for local network locations.

Near-regional distance is defined as 2.5° to 10°. Although more conventional definitions for regional distance extend to greater distance, we find a distinct increase in residual spread at 10° (Fig. 5), especially for the Sn phase. At this distance range first arriving rays travel in the crust and upper mantle, bottoming in the lithosphere. We include analysis for *regional* distances extending out to 20°, where first arrivals are interacting with upper-mantle discontinuities, causing phase misidentification and increased travel-time prediction error. Fig. 4 shows the observed travel-times derived from cluster analysis together with the AK135 predictions in the far-regional distance range. It is clear that phase misidentification errors can frequently occur, seriously effecting location accuracy.

We define *teleseismic* distance as the distance range between 28° to 91°. This distance range corresponds to bottoming depths in the lower mantle (between 740 km and 2740 km, the top of the D" layer) for AK135 P-waves. Global networks reliably record events with magnitude 4.5 or greater at teleseismic distances. In this study we exclude PKP phases from locations to avoid potential errors stemming from misidentification of PKP branches in the distance range 125° to 150°. We also exclude data in the distance range 20° to 28°, which corresponds to a bottoming depth between 660 and 760 km. As noted in Kennett and Engdahl (1991) an *ad hoc* linear gradient is used to connect the

empirically determined velocities above and below this depth range, resulting in travel times that are considered somewhat less reliable.

Fig. 5 shows the median and spread (median absolute deviation) of path corrections obtained from HDC analysis as a function of epicentral distance. Between 2.5° and 10° the spread gradually increases from about 2 seconds to about 4.5 seconds. This increase could be indicative of integration of model error over longer paths. Between 10° and 11° the spread jumps to approximately 6.5 seconds. This jump suggests prominent 3-D heterogeneities that cannot be accounted for by 1-D models and prompts us to treat the 2.5°-10° and the more traditional 2.5°-20° regional distances separately. Fig. 5 also shows that residual spread decreases between about 18° and 28° and remains constant (and low) at teleseismic distance.

3.1 GT Criteria

To derive constraints on the network geometry, we rely on parameters that are routinely reported or can be easily derived from bulletin data. We have considered criteria such as the epicentral distance to the closest station (local distance), the number of stations and phases used to locate the event, the largest azimuthal gap and secondary azimuthal gap. Each criterion is considered at local, near regional, regional, and teleseismic distance ranges. After considering each of these criteria we find that criteria related to geographic station coverage are by far the most indicative of location accuracy.

The largest azimuthal gap in station coverage is directly related to network geometry and provides a quantitative measure on how well an event is surrounded by stations. Although azimuthal gap provides reliable location accuracy in some instances, this metric is susceptible to errors at crucial stations. We find that the secondary azimuthal gap is a more robust measure of network geometry and location accuracy. Secondary azimuthal gap is defined as the largest azimuthal gap filled by a single station, illustrated in Fig. 6. If the station closing the secondary gap suffered from picking or clock errors, the location may be seriously biased. The secondary azimuthal gap criterion not only reduces vulnerability to picking and travel-time prediction errors at crucial stations, but it implicitly invokes constraints on both the azimuthal gap and the minimum number of stations.

We adopt the "ground truth" GTX classification of Bondár et al. (2001) that uses the "X" suffix to designate location accuracy in kilometers. We modify this nomenclature to $GTX_{C\%}$, where C% is the percent confidence. For example, events that are accurate to within 5 km at a 95% confidence level are designated $GT5_{95\%}$. A confidence level is more realistic than a bounding value, because we determine accuracy criteria empirically, and the possibility exists that egregious errors (clock or phase misidentification) may exist for events outside of our criteria-defining data set. For reasons discussed below, we apply accuracy criteria to epicenter parameters (latitude, longitude) only. Depth and origin time are treated separately.

3.2 Local network location accuracy criteria

The most accurate epicenters can be obtained for events inside dense, local networks. Based on our tests, crustal events are located with 5 km accuracy or better at the 95% confidence level if they are located with

- at least 10 stations within 250 km with an azimuthal gap less than 110° and a secondary azimuthal gap less than 160°
- at least one station within 30 km from the epicenter

The latter constraint gives some confidence in depth for crustal events.

To develop the selection criteria for GT5 candidate events at the 95% confidence level, two GT0 events, the 1992/11/02 ammunition storage explosion in Switzerland, and the 1999/11/11 5-ton calibration explosion in the Dead Sea, Israel, have been relocated with 10 randomly selected stations within 250 km of the epicenter. 10,000 realizations were generated for both events, and the azimuthal gap, secondary gap and number of stations within 30 km from the epicenter were measured for each Monte Carlo realization.

Fig. 7 shows the two-dimensional histograms of mislocation vs. gap (Fig. 7a) and secondary gap (Fig. 7b). It is clear that it is not possible to define constraints on the network geometry that would select all events located with 5 km accuracy or better and reject those with mislocation greater than 5 km. Therefore we specify the confidence level with which candidate GT5 events are selected. The bimodal distribution on Fig. 7a

again illustrates the importance of the notion of the secondary gap. The bimodality in the gap-mislocation distribution disappears on the secondary gap-mislocation distribution (Fig. 7b), indicating that in some network geometries a station closing a large gap can impart a significant bias into the location. As the cumulative histogram of mislocations in Fig. 8 indicates, 95% of the events identified by the GT5 selection criteria are located with better than 5 km accuracy, while the remaining 5% of events are not worse than GT10. Fig. 9 shows the distributions of the realizations satisfying the $GT5_{95\%}$ criteria (filled histograms) as a function of mislocation, depth and origin time difference relative to the true hypocenter. The $GT5_{95\%}$ selection criteria effectively cut off the long tails of the distributions obtained from all realizations (hollow histograms).

3.3 Regional network location accuracy criteria

To derive GT selection criteria for near-regional and regional networks we relocate the test GT5 data set using the modified EHB procedures, described in section 2.2. Two sets of realizations are carried out, one with a network between 2.5° and 10° and the other set with a network between 2.5° and 20°. A secondary azimuthal gap of 120° is determined to be a natural break point for both near-regional and regional networks.

Fig. 10 shows the median mislocation and spread for each 5-percentile worth of data as a function of secondary gap for distances between 2.5° and 10° (Fig. 10a) and 2.5° and 20° (Fig. 10c). The explosion population (stars) is clearly better located than the earthquakes (squares). However, near-regional networks perform considerably better for both

populations than networks spanning the whole regional distance range. The figure illustrates the case where more is less: adding stations from far-regional distances may result in less accurate locations. From the cumulative histograms of mislocations (Figs. 10b and 10d) for events with secondary gap less than 120° we conclude that the single constraint

- secondary azimuthal gap less than 120°

selects earthquakes of $GT20_{90\%}$ and explosions of $GT15_{95\%}$ when located with stations between 2.5° and 10° (near-regional distance range). For regional networks the same constraint yields $GT25_{90\%}$ for earthquakes, while the accuracy of the locations of nuclear explosions remains $GT15_{95\%}$.

3.4 Teleseismic network location accuracy criteria

For teleseismic networks we follow the same approach as for the regional case, i.e. we relocate the GT5 data set using only stations in the 28° to 91° distance range. Fig. 10e shows the median mislocation and spread versus secondary gap for distances between 28° and 91° and the corresponding cumulative distribution of mislocations (Fig. 10f). As in the regional case, earthquakes and explosions are clearly separated. We find again that

- secondary azimuthal gap less than 120°

is the dominant metric, which identifies $GT25_{90\%}$ earthquakes and $GT15_{95\%}$ explosions. It should be noted that in the GT5 data set subduction zone events are not well sampled,

and bias errors may be larger in these areas. Furthermore, the uncertainties in our GT5 data set (5 km for earthquakes) for events located by HDC analysis are propagated to the GT accuracy assessment. We note that use of a GT5 data set to validate GT20 criteria only adds 1 or 2 km of additional uncertainty if vector mislocation for the GT5 is azimuthally random.

We further validate the teleseismic criterion by performing a Monte Carlo simulation using the 1998/05/28 underground nuclear explosion in Pakistan. We believe that this explosion is a better test of location uncertainty than explosions at established test sites, where prior information about event location may bias analyst phase picking procedures. Furthermore, the unusual complexity of far-field waveforms (Barker et al., 1998) tends to complicate phase picking, similar to earthquakes.

Ten thousand realizations were generated by locating the event with random subsets of stations (between 10 and 70 out of 125) in the teleseismic distance range. We allowed for free depth solution. The two-dimensional histogram of mislocation versus secondary gap (Fig. 11a) suggests that the 120° secondary gap criterion is a reasonable choice. The cumulative histogram of mislocations (Fig. 11b) for realizations located with secondary gap less than 120° confirms the $GT25_{90\%}$ criterion. The location accuracy does not seem to depend on the number of stations (Fig. 12a) as once the number of stations required to fulfill the secondary gap criterion is reached, adding more stations only slightly reduces the secondary gap, thus leaving the relative station importances in the location process

unchanged. The location accuracy also shows a slight, almost linear dependence on estimated focal depth (Fig. 12b). However, even a depth error of 100 km results in only a 25 km mislocation, still within the GT25 category.

4 DISCUSSION

The set of criteria we have established here provide a means of estimating epicenter error which will err on the generous side. Detailed studies may significantly improve location accuracy. For example, the use of optimized models and the use of 3-dimensional earth parameterization can reduce systematic travel-time prediction error. Better models not only improve travel-time prediction accuracy, but they better satisfy the statistical assumptions outlined in the introduction. Furthermore, arrival-time errors can be reduced through careful analysis of travel-time residuals for event clusters, review of picks and waveforms, and determination of relative picks based on waveform correlation. Finally, advanced location algorithms, such as multiple event location techniques (Douglas, 1967; Dewey, 1991; Jordan and Sverdrup 1981; Engdahl and Bergman, 2001; Pavlis and Booker, 1983; Waldhauser and Ellsworth, 2000; Rodi and Toksöz, 2001), can also improve seismic location. We note however that our goal is to establish criteria for routine catalog locations that may not make use of an optimized model, detailed review of picking errors or advanced algorithms, and investigators who make use of these catalogs may not have access to the basic data needed to improve upon location accuracy.

4.1 Explosions vs. earthquakes

As we noted earlier, there is a striking difference in location accuracy between earthquakes and explosions. At regional distance the same network-coverage criteria results in $GT15_{95\%}$ for explosions and $GT20_{90\%}$ for earthquakes. At teleseismic distance $GT15_{95\%}$ degrades to $GT25_{90\%}$ for earthquakes.

There are a number of factors contributing to the location accuracy discrepancy between earthquakes and explosions. Below we provide an unordered list of possible sources of the discrepancy.

- Source finiteness, complexity and radiation patterns
- Larger picking errors for earthquake arrivals; nuclear explosions in most cases produce clear, impulsive P-arrivals and can therefore be read more accurately.
- Phase misidentification (more common for regional distance range)
- More conscientious analysis for nuclear explosions, especially at known test sites
- Earthquake reference events are not as accurate as explosion reference events
- AK135 may perform quite well at most test sites (earthquakes tend to occur at faults that are more likely to produce near-source heterogeneity)
- Origin time and depth errors may be correlated with epicenter errors for earthquakes, whereas explosions are generally fixed near the surface.

- Some subduction zone events are included in the test data set that may produce greater bias error in the earthquake population

Although each of these factors may diminish location accuracy for earthquakes, Fig 3 suggests that analyst attention to nuclear explosions is a significant factor. In each distance range the statistical mode (established by the small-residual population for explosions) of the travel-time residuals was significantly closer to zero for explosions than for earthquakes, suggesting that *a priori* information aided in phase identification. If this is true, then location accuracy should not be established using catalog arrival times for test-site explosions. Although many arrival-time picks appear to be aided by predicted travel-time, the shoulders in residual populations for near-regional and regional distances indicate the presence of systematic path anomalies (slower propagation to Californian stations from the Nevada Test Site, and faster propagation through the Russian platform from Novaya Zemlya and Semipalatinsk). Path anomalies are not at evident in the earthquake population because a greater diversity of path anomalies fills out the distribution and reduced location accuracy adds to the variance of the distribution.

4.2 Depth and origin time

For many applications event depth and origin time are as important as epicenter. However, unlike epicenter parameters, depth and origin time estimates are strongly dependent on the velocity model, hindering development of network-geometry-based accuracy criteria.

We use the geometry of the Racha, Georgia aftershock sequence (Fuenzalida et al., 1993) to test the sensitivity of velocity model error on local-network location errors (Myers and Schultz, 2000a). We generate synthetic arrivals using a simple velocity model, then perturb the velocity model and relocate the events (Fig. 13). We see that for this realistic network geometry, epicenter accuracy is maintained, with mislocation of only about 0.5 km (when only P-waves are used). However, depth can be systematically shifted up to 5 km kilometers and origin time is shifts in excess of 0.6 seconds occur in response to bulk velocity model error. We find that inclusion of S-arrivals reduces the origin time and depth error, but degrades epicenter accuracy, although depth and origin time errors remain larger than epicenter errors.

Estimation of focal depth based on phase arrival times from regional and teleseismic networks is difficult at best. Although arrival times of surface-reflected phases (e.g. pP, sP) can be used to improve depth estimation, surface-reflected phases for events in the shallow crust (as well as pwP in the case of sub-oceanic events) are commonly convolved into one group arrival, complicating analyst efforts to pick phase onsets. As a result of these complications, depth phases are reported for only half of all ISC events, including deep events. Even when surface-reflected arrivals are clear, phase identification can be problematic. Engdahl et al. (1998) find that re-identification of these phases (for events at all depths) based on likelihood of arrival time significantly improves catalog consistency, suggesting that surface-reflected phases are often misidentified. Moreover, a

large number of phases reported by the ISC with no phase identification could be associated as depth phases or PcP.

Regional and teleseismic estimation of focal depth is poorly constrained by direct phases. Fig. 14 shows that travel-time residuals are relatively insensitive to large changes in event depth, when compared to other location parameters. Because residual sensitivity to depth error is distance dependent, depth accuracy criteria should be based on distance coverage. However, we do not establish such a criteria here, because we do not have ground-truth data to validate the approach.

We note that even when surface-reflected phases are used to constrain depth, origin time is still poorly resolved due to the dependence on travel-time prediction error. If depth or reflected phases (PmP, PcP) are not used to constrain depth, then depth and origin time error are almost perfectly correlated and the accuracy of neither parameter can be assessed.

5 CONCLUSIONS

A wide variety of seismic studies – seismic hazard analysis, regional and teleseismic tomography to derive 3D velocity models of the Earth, and location calibration – depend on commonly available catalog information. However, the results can only be as good as the input data set. We recognize the need to establish location accuracy criteria based on parameters that are readily available or can be easily extracted from catalog data. Epicenter accuracy can be assessed using constraints on network geometry. We find the

most useful and easiest to derive parameters that are correlated with epicenter accuracy are azimuthal gap and secondary azimuthal gap, which are related to network coverage. Secondary azimuthal gap is a more robust measure for epicenter accuracy than primary azimuthal gap, but in the case of local network locations the primary and secondary azimuthal gap are both utilized to achieve $GT5_{95\%}$.

Event depth and origin time accuracy are linked to travel-time prediction accuracy, which depends on the accuracy of the velocity model used to develop the catalog. Since the quality of the velocity model is difficult to assess from the catalogs themselves, we did not attempt to develop criteria for the general assessment of accuracy of these parameters.

We identified three distance ranges - local (0° - 2.5°), near-regional (2.5° - 10°) and teleseismic (28° - 91°) for which reliable criteria can be developed. These distance ranges are the least prone to reading errors and phase misidentification as well as lateral inhomogeneities not modeled by the underlying 1D models used to produce the catalogs.

We used GT0 to develop and validate $GT5_{95\%}$ criteria for local network locations. However, in regional and teleseismic distance ranges the earthquake and explosion populations are dramatically separated with regard to location accuracy. We found that for any station coverage, earthquakes are not as well located as explosions, and the difference in accuracy is about 5-10 km. Thus, using GT0 nuclear explosions at established test sites to derive GT selection criteria would lead to overly optimistic results. To avoid this caveat, we used a well-located GT5 data set of earthquakes to

establish criteria for the regional and teleseismic ranges. The criteria withstand further validation using the GT5 1998/05/28 underground nuclear explosion in Pakistan.

The epicenter accuracy criteria for the various distance ranges are given below. Note that subduction zone events may have a larger location uncertainty due to the travel-time bias introduced by the subducting slab, even if the station coverage satisfies the GT selection criteria. Therefore the events identified by the criteria below should only be considered as ground truth candidates.

Local networks (0° - 2.5°)

- At least 10 stations within 250 km with an azimuthal gap less than 110° and a secondary azimuthal gap less than 160° and at least one station within 30 km from the epicenter provides $GT5_{95\%}$

Near-regional networks (2.5° - 10°)

- secondary azimuthal gap less than 120° results in $GT20_{90\%}$

Regional networks (2.5° - 20°)

- secondary azimuthal gap less than 120° results in $GT25_{90\%}$

Teleseismic networks (28° - 91°)

- secondary azimuthal gap less than 120° results in $GT25_{90\%}$

ACKNOWLEDGMENTS

We thank Bob North and Keith McLaughlin as well as the anonymous reviewers whose comments helped to improve the paper. This work was supported by the Defense Threat Reduction Agency under contracts DTRA01-00-C-0013 and DTRA01-00-C-0032 and the Department of Energy under contract W-7405-ENG-48.

REFERENCES

Albright, D., Gay, C. & Pabian, F., 1998. New details emerge on Pakistan's nuclear test site, EOM. http://www.modernag.com/Common/Archives/DecemberJan/gay.htm

Antolik, M, Ekström, G. & Dziewonski, A.M., 2001. Three-dimensional Models of Mantle P-wave velocity, *Pure Appl. Geophys.*, **158**, 291-317.

Barker, B., Clark, M., Davis, P., Fisk, M., Hedlin, M., Israelsson, H., Khalturin, V., Kim, W-Y., McLaughlin, K., Meade, C., Murphy, J., North, R., Orcutt, J., Powell, C., Richards, P., Stead, R., Stevens, J., Vernon, F. & Wallace, T., 1999. Monitoring nuclear tests, *Science*, **281**, 1967-1968.

Bondár, I., Yang, X., North, R.G. & Romney, C., 2001. Location Calibration Data for CTBT Monitoring at the Prototype International Data Center, *Pure Appl. Geophys.*, **158**, 19-34.

Bondár, I., Engdahl, E.R., Israelsson, H., Yang, X., Hofstetter, A., Ghalib, H., Gupta, I., Wagner, R., Kirichenko, V. & McLaughlin, K., 2002. Status of Reference Event Collection for Western Eurasia, the Middle East, Northern Africa and Europe - The

Group 2 Location Calibration Consortium Reference Event List 2.0 Delivery, *4th Location Calibration Workshop*, Oslo, Norway. http://g2calibration.cmr.gov/calibration/Presentations/Oslo_2002/Oslo2002_bondar.pdf

Buland, R., 1986. Uniform reduction error analysis, *Bull. Seismol. Soc. Am.*, **76**, 217-230.

Dewey, J.W., 1991. Joint epicenter determination for earthquakes occurring over several decades: a case history from Northern Algeria, *in Seismicity, Seismotectonics and Seismic Risk of the Ibero-Maghreb Region*, eds. Mezcua, J. & Udias, A., Instituto Geografico Nacional, Monografia No. 8, Madrid, Spain, 51-63.

Dewey, J.W., Herron, E. & Kork, J.O., 1999. Recent Calibration Events in the United States, *21st Seismic Research Symposium*, 48-57. http://www.cmr.gov/srs/srs1999/papers1/dewey.pdf

Dewey, J.W. & Kork, J.O., 2000. Selection of Earthquakes for Calibration Events in the United States, *2nd Workshop on Location Calibration*, Oslo, Norway.

Douglas, A., 1967. Joint Epicentre Determination, *Nature*, **215**, 47-48.

Engdahl, E.R., van der Hilst, R. & Buland, R. 1998. Global Teleseismic Earthquake Relocation with improved Travel Times and Procedures for Depth Determination, *Bull. Seism. Soc. Am.*, **88**, 722-743.

Engdahl, E.R. & Bergman, E.A., 2000. Identification and validation of Reference Events within the area being regionally monitored by IMS stations in Asia and North Africa,

22nd Seismic Research Symposium, New Orleans, USA. http://www.cmr.gov/srs/srs2000/papers/02-13.pdf

Engdahl, E.R. & Bergman, E.A., 2001. Validation and generation of reference events by cluster analysis, *23rd Seismic Research Review,* Jackson Hole, USA. http://www.cmr.gov/srs/srs2001/Screen/02-09.pdf

Evernden, J., 1969. Precision of epicenters obtained by small numbers of world-wide stations, *Bull. Seism. Soc. Am.*, **59**, 1365-1398.

Flinn, E., 1965. Confidence regions and error determinations for seismic event location, *Rev. Geophys.*, **3**, 157-185.

Fuenzalida, H., Rivera, L., Haessler, H., Legrand, D., Philip, H., Dorbath, L., McCormack, D., Arefiev, D., Langer, C. & Cisternas, A., 1997. Seismic source study of the Racha-Dzhava (Georgia) earthquake from aftershocks and broadband teleseismic body-wave records: and example of active nappe tectonics, *Geophys. J. Int.*, **130**, 29-64.

Gitterman, Y. & Shapira, A., 2001. Dead Sea seismic calibration experiment contributes to CTBT monitoring, *Seism. Res. Lett.*, **72**, 159-170.

Herrin, E., 1968. Introduction to 1968 seismological tables for P phases, *Bull. Seism. Soc. Am.*, **58**, 1193-1195.

Herrin, E. & Taggart, J., 1968. Source bias in epicenter determinations, *Bull. Seism. Soc. Am.*, **58**, 1791-1796.

Israelsson, H., Engdahl, E.R. & Bergman, E.A., 2001. Cross validation of two methods for event cluster analysis, Group 2 Phase 1 Delivery Document, http://g2calibration.cmr.gov/calibration/files/hjd-hdc-validation.pdf.

Jordan, T.H. & Sverdrup, K.A., 1981. Teleseismic location techniques and their application to earthquake clusters in the South-central Pacific, *Bull. Seism. Soc. Am.*, **71**, 1105-1130.

Kennett, B. & Engdahl, E.R., 1991. Travel Times for Global Earthquake Location and Phase Identification, *Geophys. J. Int.*, **105**, 429-465.

Kennett, B.L.N., Engdahl, E.R. & Buland, R., 1995. Constraints on seismic velocities in the Earth from travel times, *Geophys. J. Int.*, **122**, 108-124.

McLaughlin, K., Yang, X., Bondár, I., Bhattacharyya, J., Israelsson, H., Kirichenko, V., Kraev, Y., Engdahl, E.R., Ritzwoller, M., Levshin, A., Shapiro, N., Barmin, M., Antolik, M., Dziewonski, A., Ekström, G., Gupta, I., Wagner, R., Hofstetter, A., Shapira, A. & Laske, G., 2002. Improved seismic event location in Europe, Middle East, North Africa and Western Asia using 3D model-based regional travel-times, *Seism. Res. Let.*, **73**, 216.

McLaughlin, K., Bondár, I., Yang, X., Bhattacharyya, J., Israelsson, H., R. North, Kirichenko, V., Engdahl, E.R., Ritzwoller, M., Levshin, A., Shapiro, N., Bergman, E., Antolik, M., Dziewonski, A., Ekström, G., Ghalib, H., Gupta, I., Wagner, R., Chan, W., Rivers, W., Hofstetter, A., Shapira, A. & Laske, G., 2002. Seismic location calibration in

the Mediterranean, North Africa, Middle East and Western, *24th Seismic Research Review*, Pointe Vedra Beach, USA. http://www.cmr.gov/srs/srs2002/screen/02-10.pdf

Myers, S.C. & Schultz, C.A., 2000a. Calibration of seismic travel time using events with seismically determined locations and origin times, *EOS Trans. AGU*, **81**, F845.

Myers, S.C. & Schultz, C.A., 2000b. Improving sparse network seismic location with Bayesian kriging and teleseismically constrained calibration events, *Bull. Seism. Soc. Am.*, **90**, 199-211.

Myers, S.C, & Shultz, C.A., 2001. Statistical Characterization of Reference Event Accuracy, *Seism. Res. Let.*, **72**, 244.

Pavlis, G.L. & Booker, J.R., 1983. Progressive multiple event location (PMEL), *Bull. Seism. Soc. Am.*, **73**, 1753-1777.

Ritzwoller, M.H., Shapiro, N.M., Levshin, E.A., Bergman, E.A. & Engdahl, E.R., 2002. Assessment of global 3-D models based on regional ground-truth locations and travel-times, submitted to *J. Geophys. Res.*

Rodi, W. & Toksöz, M.N., 2001. Uncertainty analysis of seismic event location, *23rd Seismic Research Review*, Jackson Hole, USA. http://www.cmr.gov/srs/srs2001/02-22.pdf

Rodi, W., Engdahl, R., Bergman, E., Waldhauser, F., Pavlis, G., Israelsson, H., Dewey, J. & Toksöz, M., 2002. A new grid-search multiple event location algorithm and a

comparison of methods, *24th Seismic Research Review*, Pointe Vedra Beach, USA. http://www.cmr.gov/srs/srs2002/screen/02-19.pdf

Sambridge, M. & Kennett, B.L.N., 2001. Seismic event location: Nonlinear inversion using a neighbourhood algorithm, *Pure Appl. Geophys*., **158**, 241-257.

Steck, L.K, Velasco, A.A., Cogbill, A.H. & Patton, H.J., 2001. Improving regional seismic event location in China, *Pure Appl. Geophys*., **158**, 211-240.

Sweeney, J.J., 1996. Accuracy of Teleseismic Event Locations in the Middle East and North Africa, *Lawrence Livermore National Laboratory*, UCRL-ID-125868.

Sweeney, J.J., 1998. Criteria for Selecting Accurate Event Locations from NEIC and ISC Bulletins, *Lawrence Livermore National Laboratory*, UCRL-JC-130655.

Waldhauser, F. & Ellsworth, W.L., 2000. A double-difference earthquake location algorithm: Method and application to the Northern Hayward fault, California, *Bull. Seism. Soc. Am.*, **90**, 1353-1368.

Yang, X., North, R.G. & Romney, C., 2000. CMR Nuclear Explosion Database (Revision 3), *Center for Monitoring Research*, CMR-00/16.

FIGURE CAPTIONS

Fig. 1. Local network geometry (triangles) of a) the 1999/11/11 Dead Sea calibration explosion and b) the 1992/11/02 ammunition storage explosion in Switzerland. The 30 and 25 km circles around the epicenters (stars) are also drawn.

Fig 2. Locations of events in the test GT5 database used in this study.

Fig. 3 Travel-time residual distributions of first arriving P-waves from earthquake and explosion clusters in the test GT5 database (corrected for cluster time baseline shifts). a) earthquakes, near-regional distance range (2.5° to 10°); b) explosions, near-regional distance range; c) earthquakes, regional distance range (2.5° to 20°); d) explosions, regional distance range; e) earthquakes, teleseismic distance range (28° to 91°); f) explosions, teleseismic distance range.

Fig. 4 Reduced (relative to 8.0 km/s) Pn (white) and P (black) empirical path anomalies in the far-regional distance range derived from HDC analysis of clustered events. Repeated ray-paths provide an estimate of the median and spread of the observed travel-times from cluster to station. Travel times are corrected for cluster time baseline shifts with respect to AK135. AK135 predicted Pn and P travel time branches are also shown.

Fig. 5 Median and spread of path corrections for earthquakes in the test GT5 database derived from HDC analysis between 0° and 100°, binned in 2° intervals. The spread is fairly well behaved in near-regional and teleseismic distance ranges, but increases sharply beyond 10° in regional distances.

Fig. 6 Illustration of primary and secondary azimuthal gaps. The recording stations (triangles) are plotted for the 1975/8/23 underground nuclar explosion (star) in Novaya Zemlya. The shaded areas show the azimuthal gap (left) and the secondary azimuthal gap (right). Although the 82º azimuthal gap indicates a quite decent coverage, any reading error at HKC that provides the 160º secondary azimuthal gap may bias the location.

Fig. 7 Histograms of mislocation vs. a) azimuthal gap and b) secondary gap obtained from a Monte Carlo simulation of relocating the 1999/11/11 Dead Sea calibration explosion and the 1992/11/02 ammunition storage explosion in Switzerland with 10 randomly selected stations within 250 km from the epicenter.

Fig. 8 Percentile plots of mislocations showing all realizations (dotted line) and those satisfying the $GT_{95\%}$ local network criteria (solid line). The worst mislocation for events identified by the selection criteria is 10 km.

Fig. 9 Distributions of a) mislocation, b) origin time and c) depth for all realizations (solid lines) and for the realizations that met the $GT_{95\%}$ local network criteria. The criteria effectively cut off the heavy tails of the distributions.

Fig. 10 Mislocation by near-regional, regional and teleseismic networks. a) median of mislocation vs. secondary gap for explosions (stars) and earthquakes (squares) between 2.5° and 10°; b) percentile plot of mislocation for earthquakes (solid line) and explosions (dotted line) with secondary gap less than 120° in the near-regional distance range; c) same as a) but for the regional distance range 2.5° - 20°; d) same as b) but for the regional distance range 2.5° - 20°; e) same as a) but for the teleseismic distance range 28° - 91°; f) same as b) but for the teleseismic distance range 28° - 91°.

Fig. 11 Monte Carlo simulation of teleseismic networks using the 1998/05/28 underground nuclear explosion in Pakistan. a) histogram of mislocation vs. secondary gap; b) percentile plot of mislocations showing all realizations (dotted line) and those with secondary gap less than 120° (solid line).

Fig. 12 Mislocation as a function of a) number of stations and b) depth for teleseismic networks obtained from the Monte Carlo simulation.

Fig. 13 Simulation of the Racha aftershock sequence uses a real network geometry to test the sensitivity of local-network locations to velocity model error. For eleven events with excellent network coverage, we generate synthetic arrival times for P and S phases using a velocity model with bulk P-wave velocity of 6.2 km/s (Vp/Vs=1.73). We then change the bulk velocity and relocate the events. a) The network coverage is excellent for our test cases; triangles are seismic stations. b,

c, d) Origin time, depth and epicenter errors for relocations using only P-waves (circles) and P- and S-waves (triangles), respectively (see text for discussion).

Fig. 14 Travel-time residuals resulting from errors in event depth are compared to the overall residual spread. a) Benchmark epicenter locations (stars) are determined with local networks (aftershock deployments). Epicenters are fixed at the local-network locations to minimize errors due to lateral mislocation. Origin time is determined for depths of 0 km and 30 km using teleseismic P-wave arrivals (small triangles are teleseismic stations). b) The difference in travel-time residuals for 0 km and 30 km depths (black) are plotted with the residual population for 0 km depth locations (gray). Residual error caused by a 30 km change in depth is difficult to resolve when viewed against the overall residual spread. The small change in travel-time residual with large changes in event depth shows the difficulty of determining depth (see text for discussion).

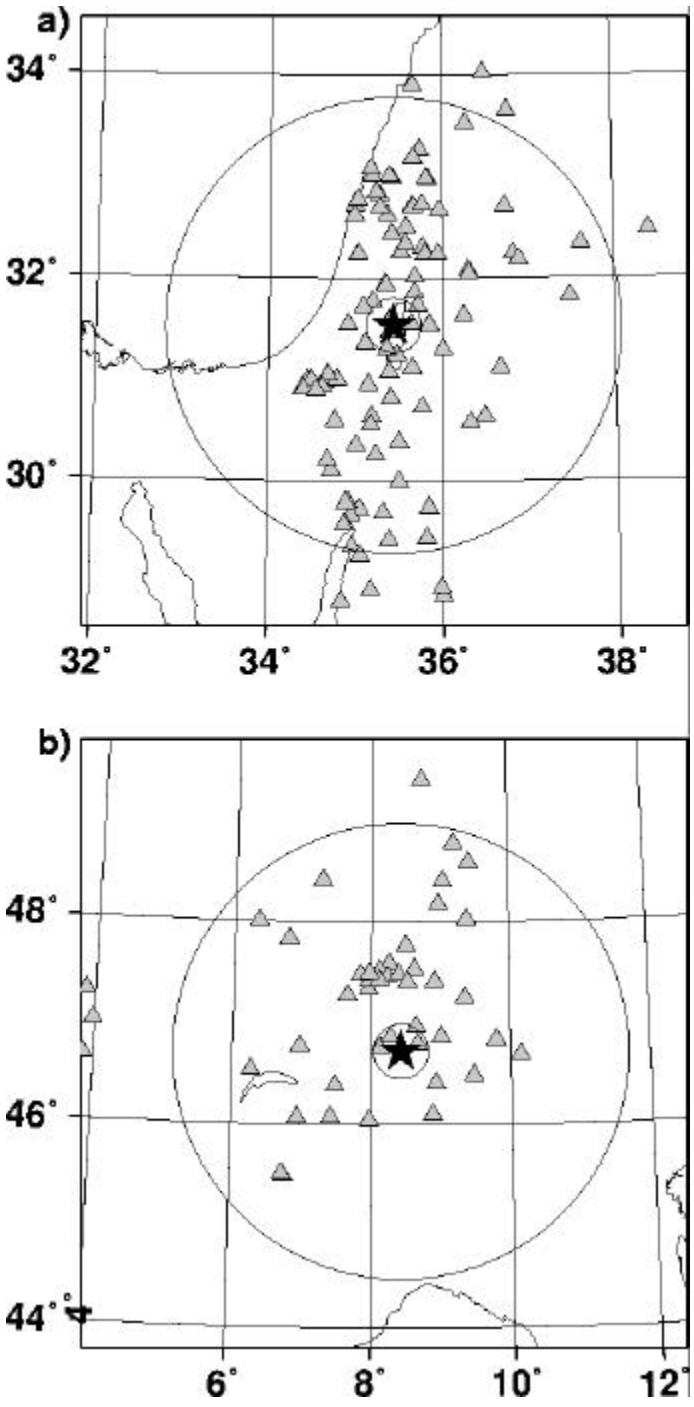

Fig. 1

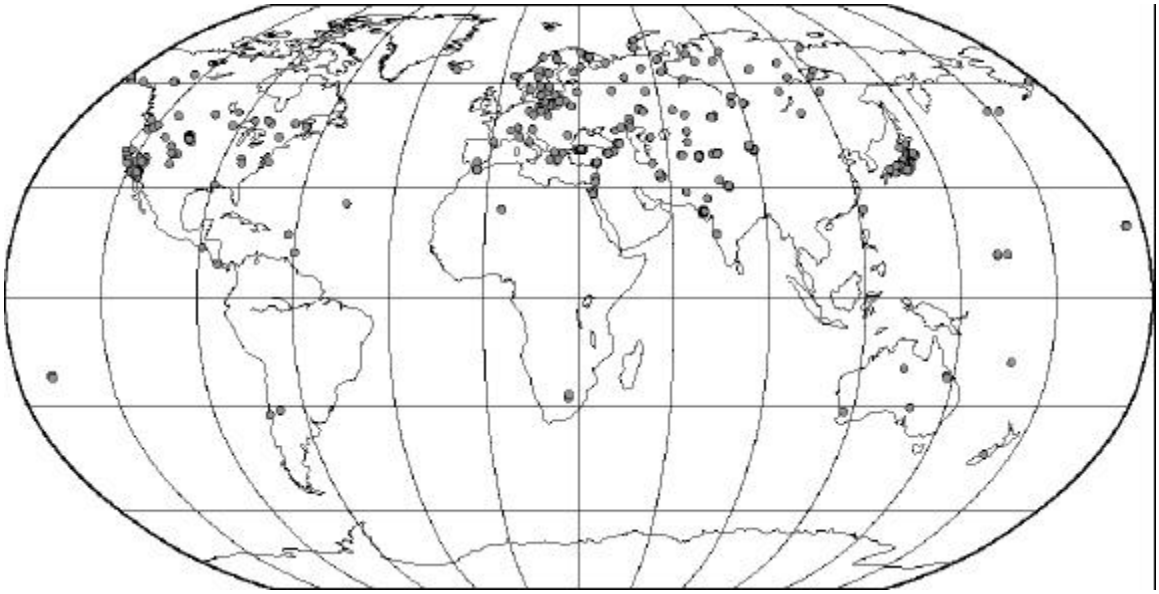

Fig. 2

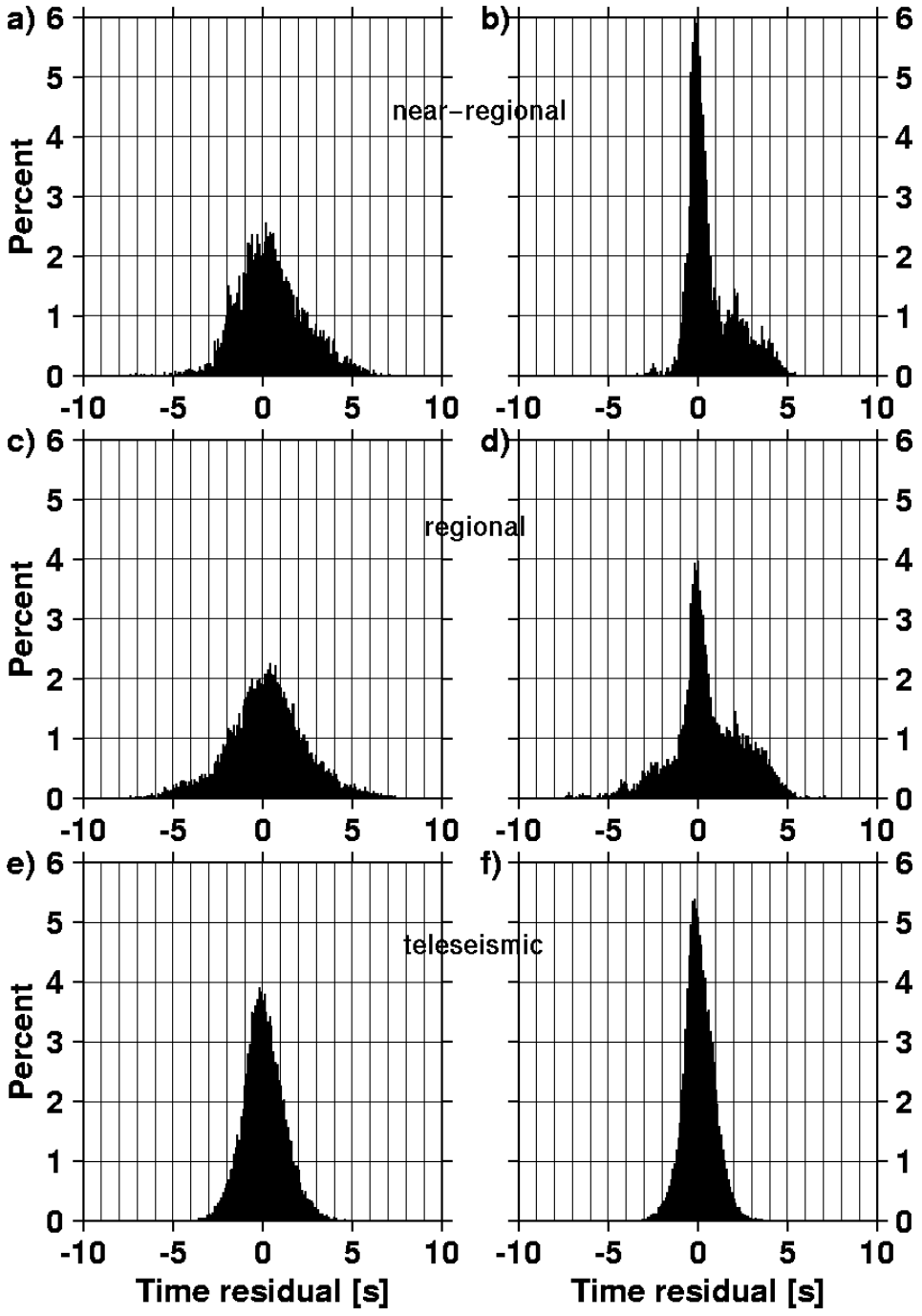
a)
b)
c)
d)
e)
f)
near−regional
regional
teleseismic
Percent
Time residual [s]
0
1
2
3
4
5
6
-10
-5
0
5
10

Fig. 3

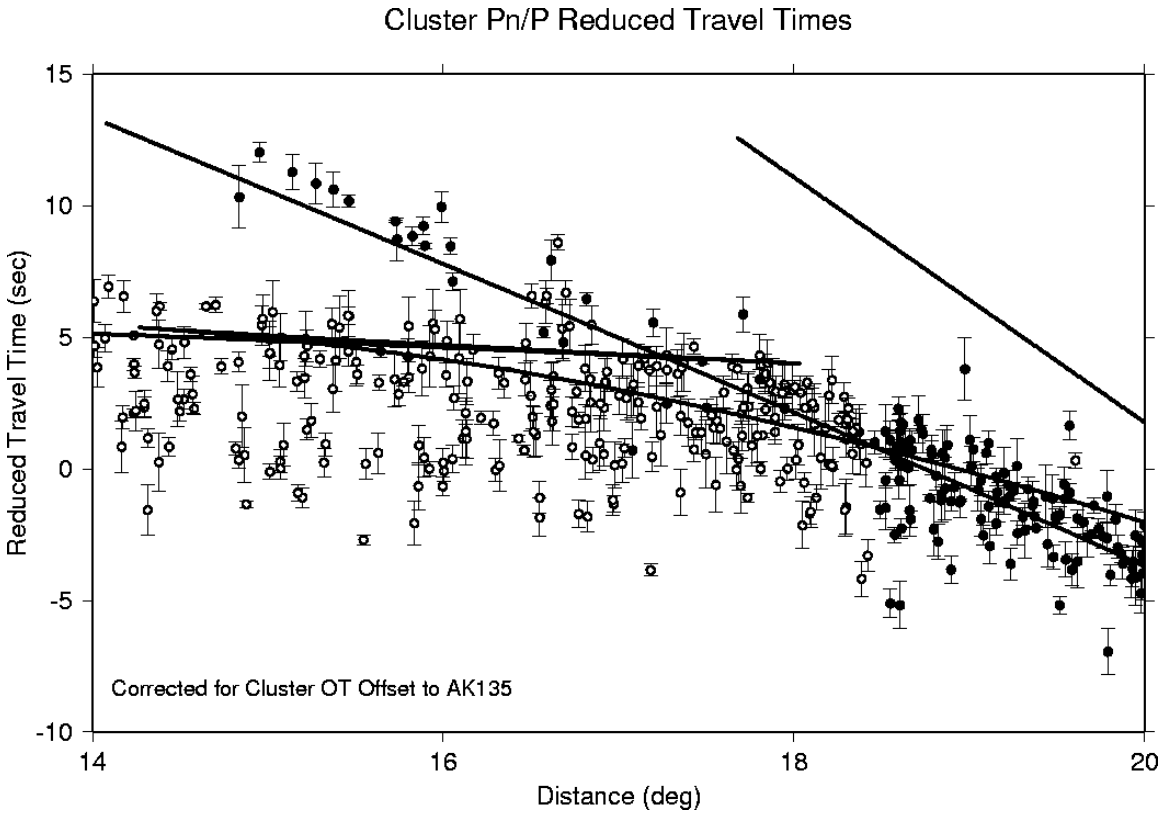
Cluster Pn/P Reduced Travel Times
Reduced Travel Time (sec)
Distance (deg)
Corrected for Cluster OT Offset to AK135
15
10
5
0
-5
-10
14
16
18
20

Fig. 4

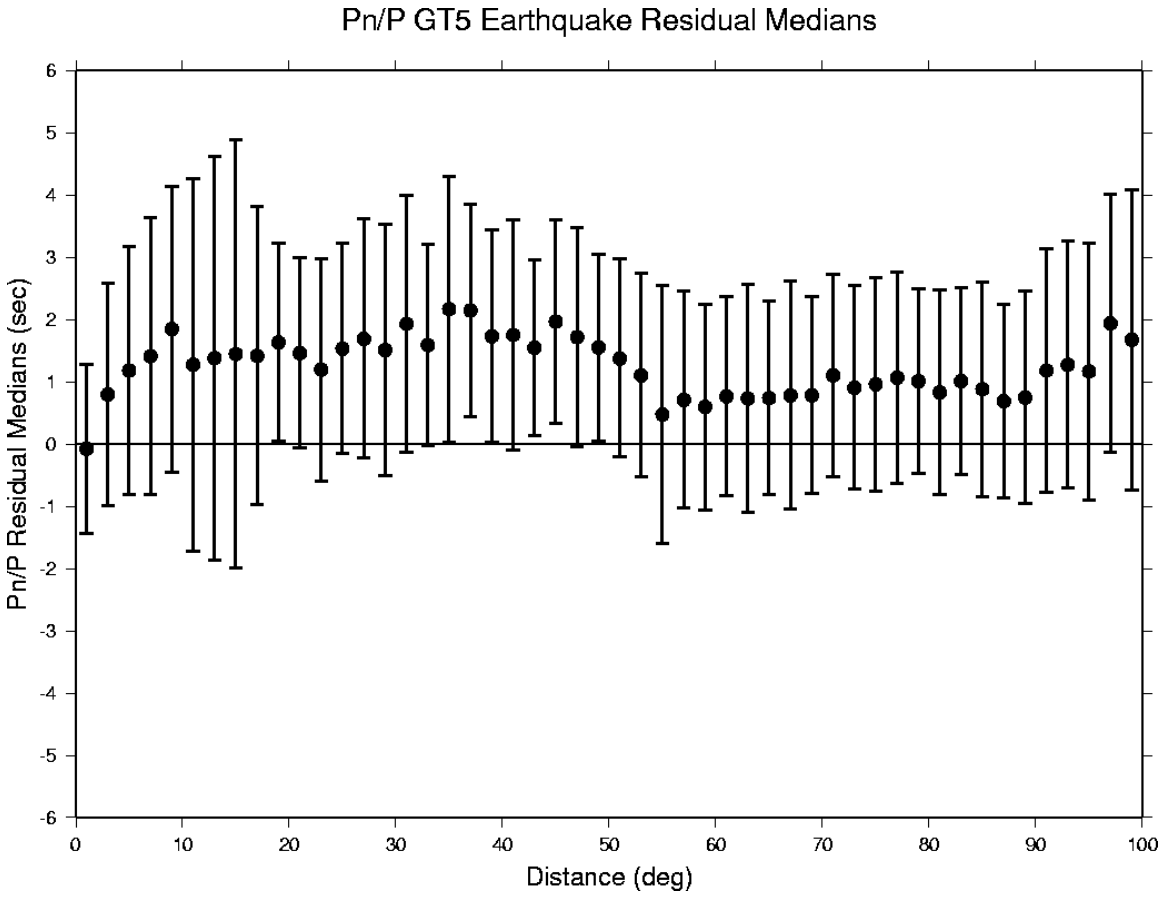
Pn/P GT5 Earthquake Residual Medians
Pn/P Residual Medians (sec)
Distance (deg)
6
5
4
3
2
1
0
-1
-2
-3
-4
-5
-6
0
10
20
30
40
50
60
70
80
90
100

Fig. 5

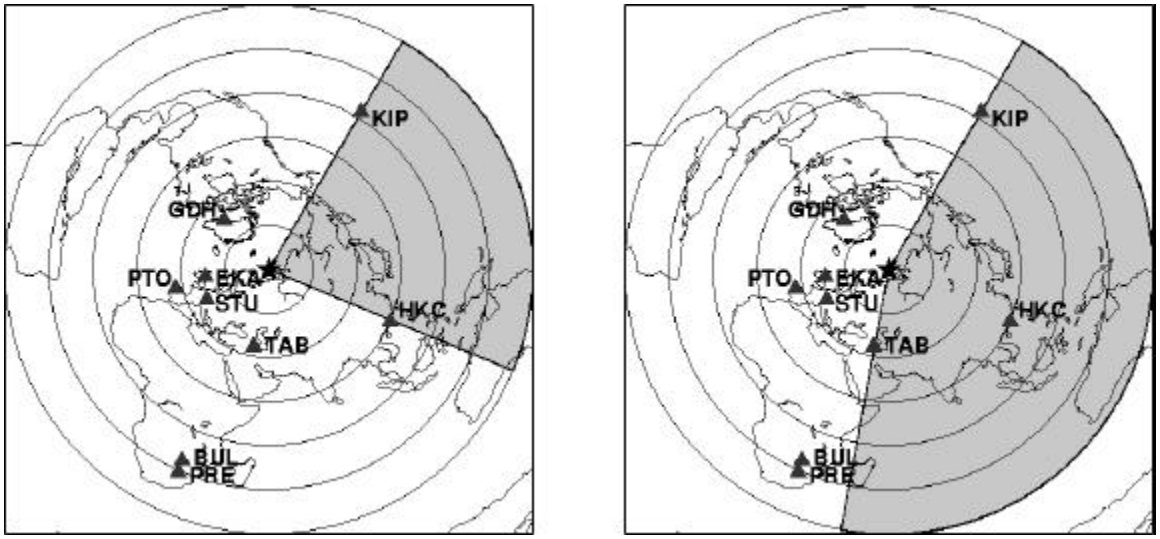
KIP
GDH
PTO
EKA
STU
HKC
TAB
BUL
PRE
KIP
GDH
PTO
EKA
STU
HKC
TAB
BUL
PRE

Fig. 6

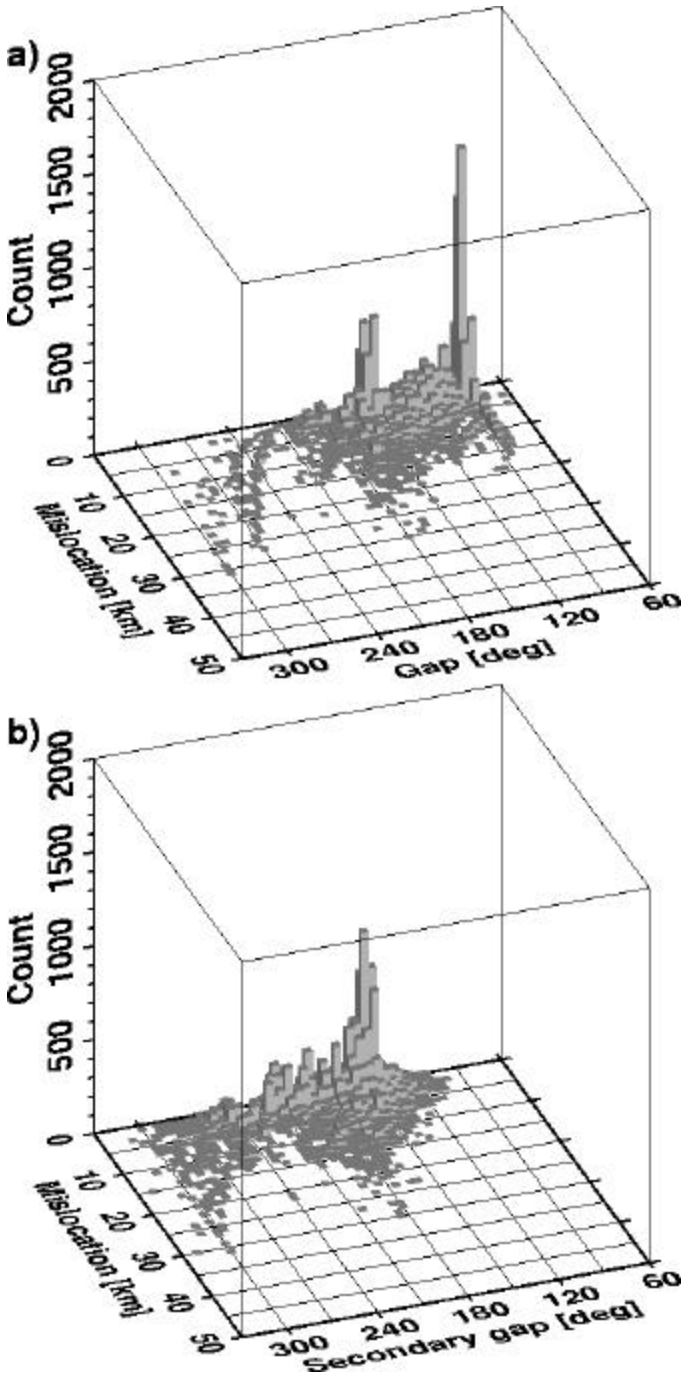
a)
Count
0
500
1000
1500
2000
Mislocation [km]
10
20
30
40
50
300
240
180
120
60
Gap [deg]
b)
Count
0
500
1000
1500
2000
Mislocation [km]
10
20
30
40
50
300
240
180
120
60
Secondary gap [deg]

Fig. 7

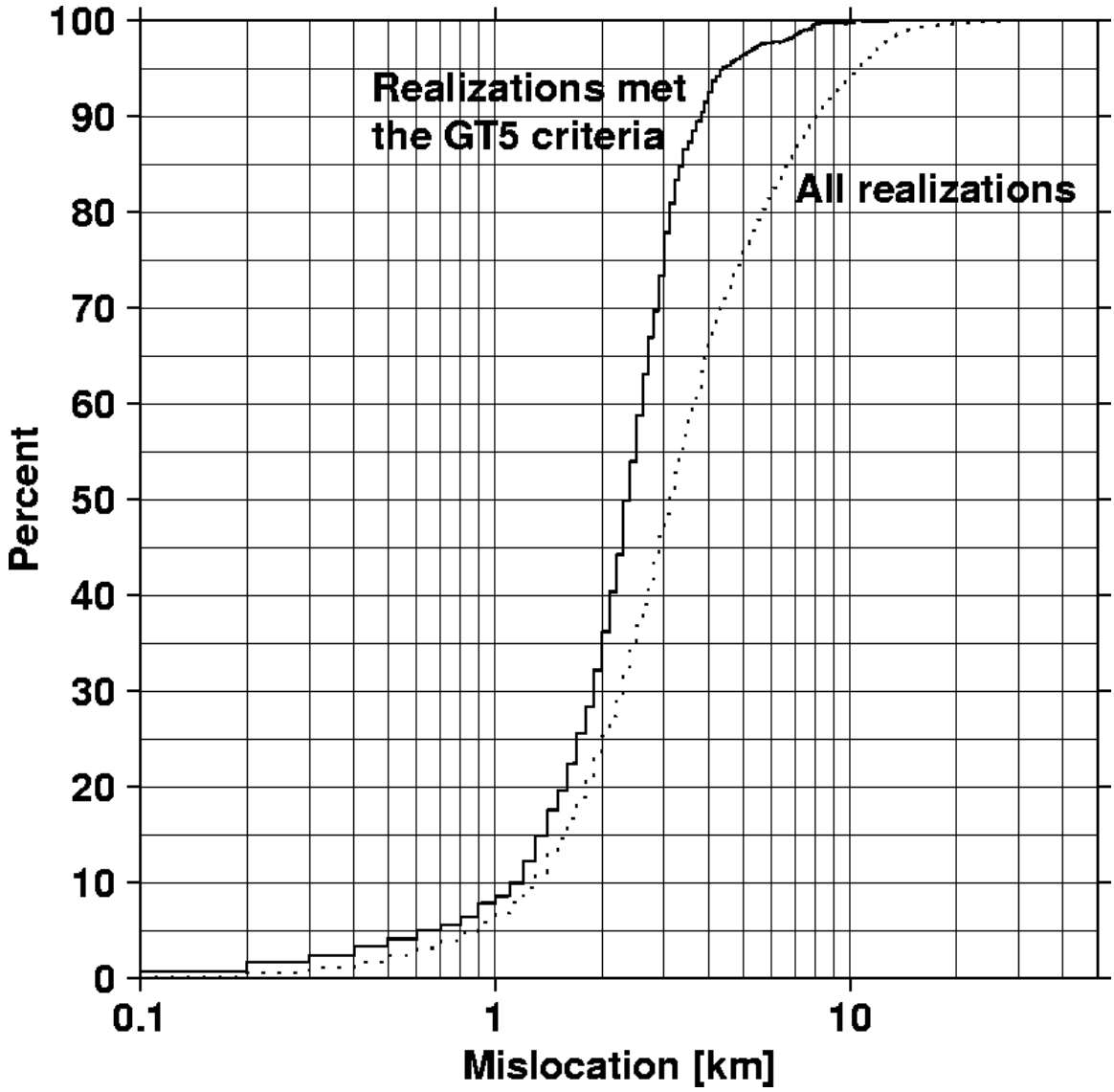
Realizations met
the GT5 criteria
All realizations
Percent
100
90
80
70
60
50
40
30
20
10
0
0.1
1
10
Mislocation [km]

Fig. 8

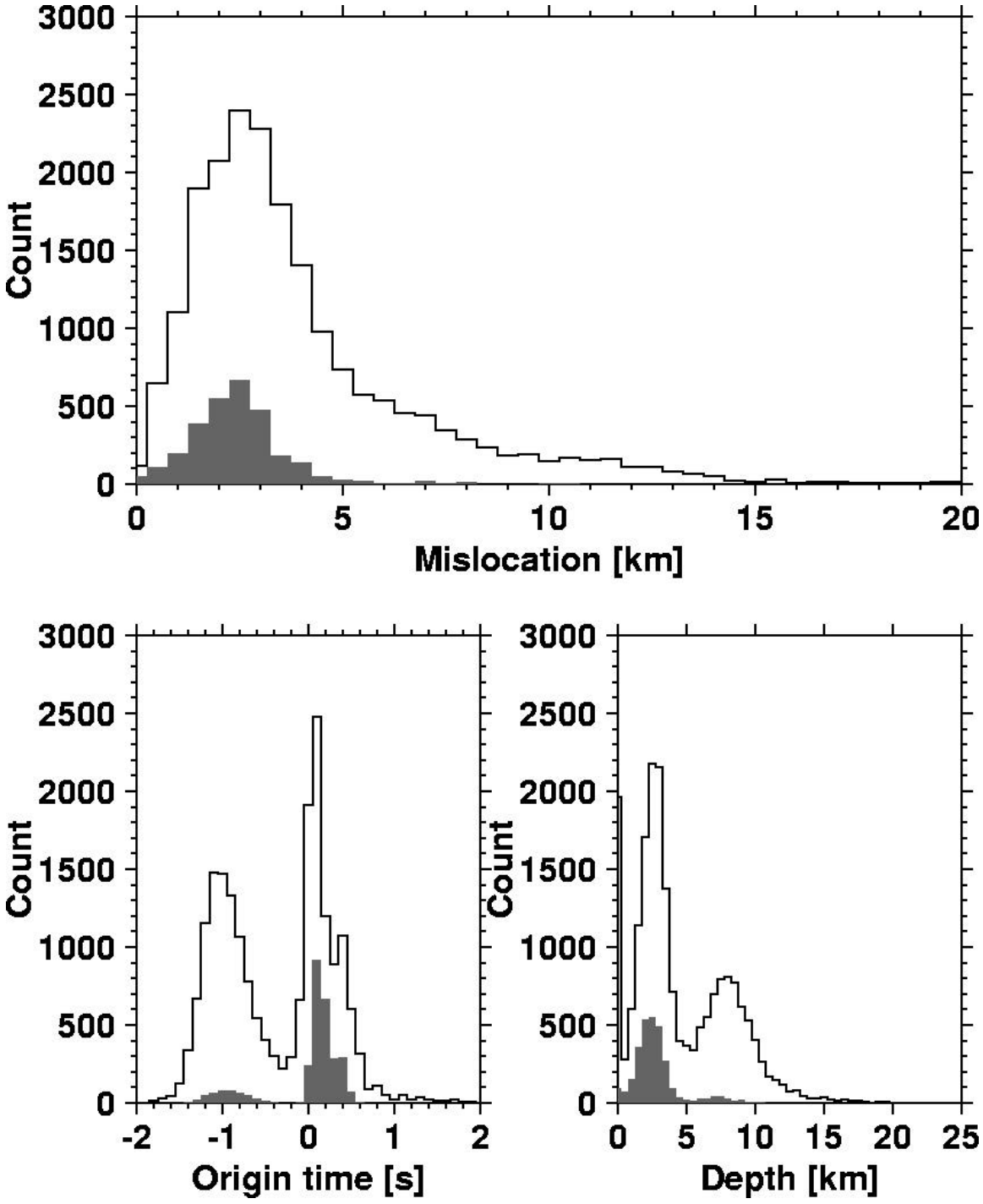
3000
2500
2000
1500
1000
500
0
Count
0
5
10
15
20
Mislocation [km]
3000
2500
2000
1500
1000
500
0
Count
-2
-1
0
1
2
Origin time [s]
3000
2500
2000
1500
1000
500
0
Count
0
5
10
15
20
25
Depth [km]

Fig. 9

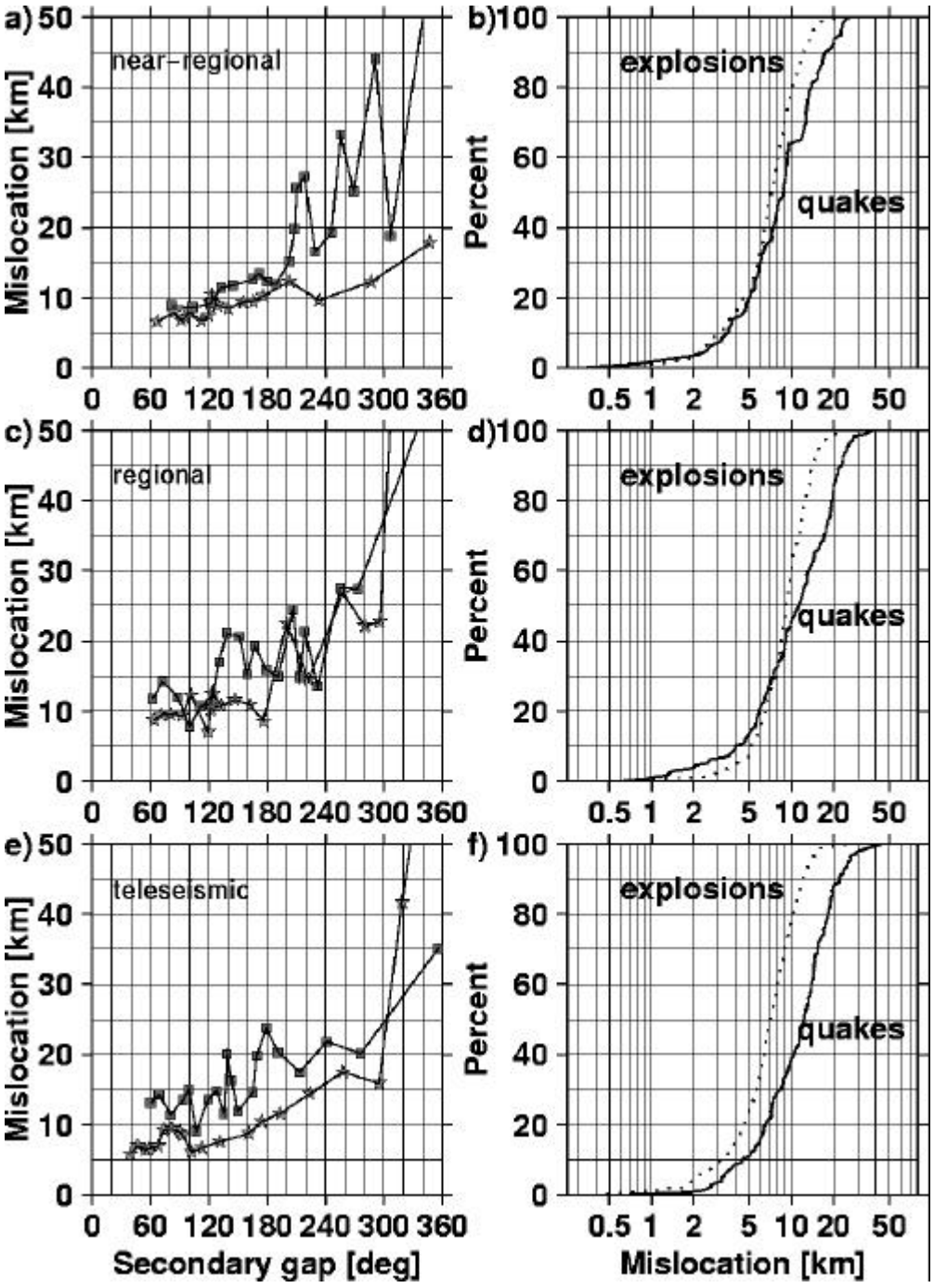
a)
near-regional
Mislocation [km]
0
10
20
30
40
50
0 60 120 180 240 300 360
b)
explosions
quakes
Percent
0
20
40
60
80
100
0.5 1 2 5 10 20 50
c)
regional
Mislocation [km]
d)
explosions
quakes
Percent
e)
teleseismic
Mislocation [km]
Secondary gap [deg]
f)
explosions
quakes
Percent
Mislocation [km]

Fig. 10

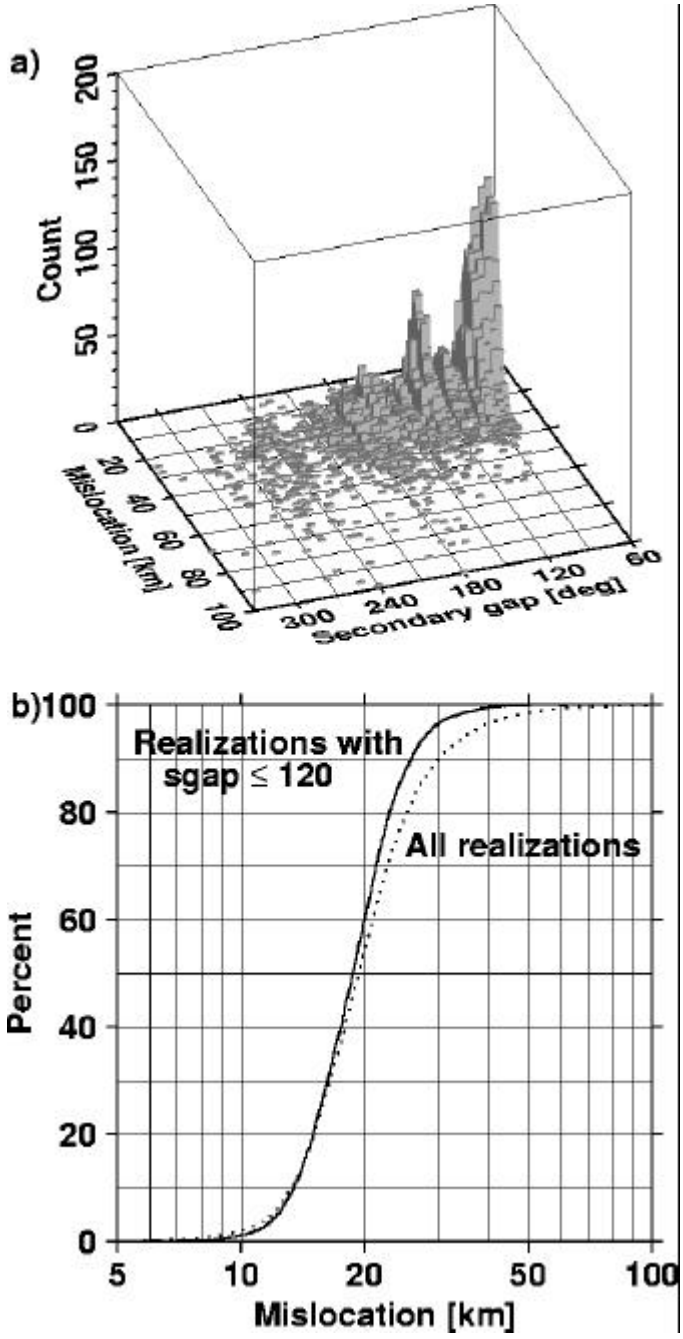
a)
Count
0
50
100
150
200
Mislocation [km]
20
40
60
80
100
300
240
180
120
60
Secondary gap [deg]
b)100
Realizations with
sgap ≤ 120
All realizations
Percent
0
20
40
60
80
5
10
20
50
100
Mislocation [km]

Fig. 11

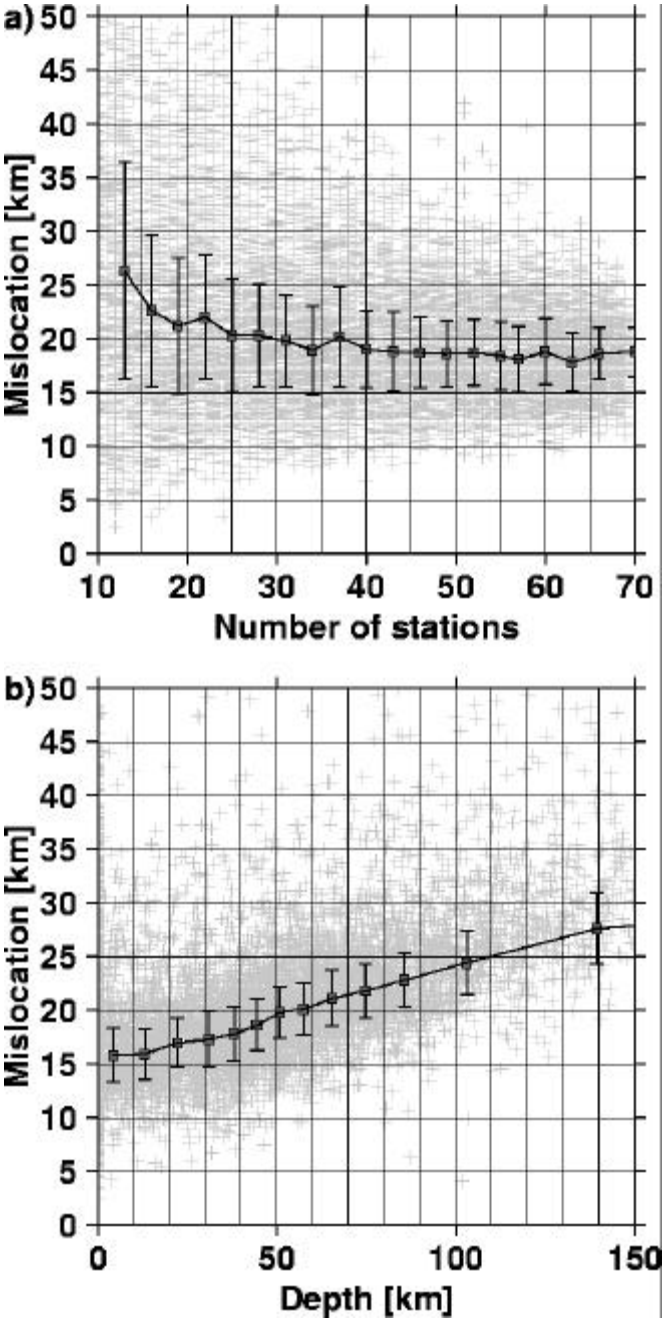
a)
Mislocation [km]
0
5
10
15
20
25
30
35
40
45
50
10
20
30
40
50
60
70
Number of stations
b)
Mislocation [km]
0
5
10
15
20
25
30
35
40
45
50
0
50
100
150
Depth [km]

Fig. 12

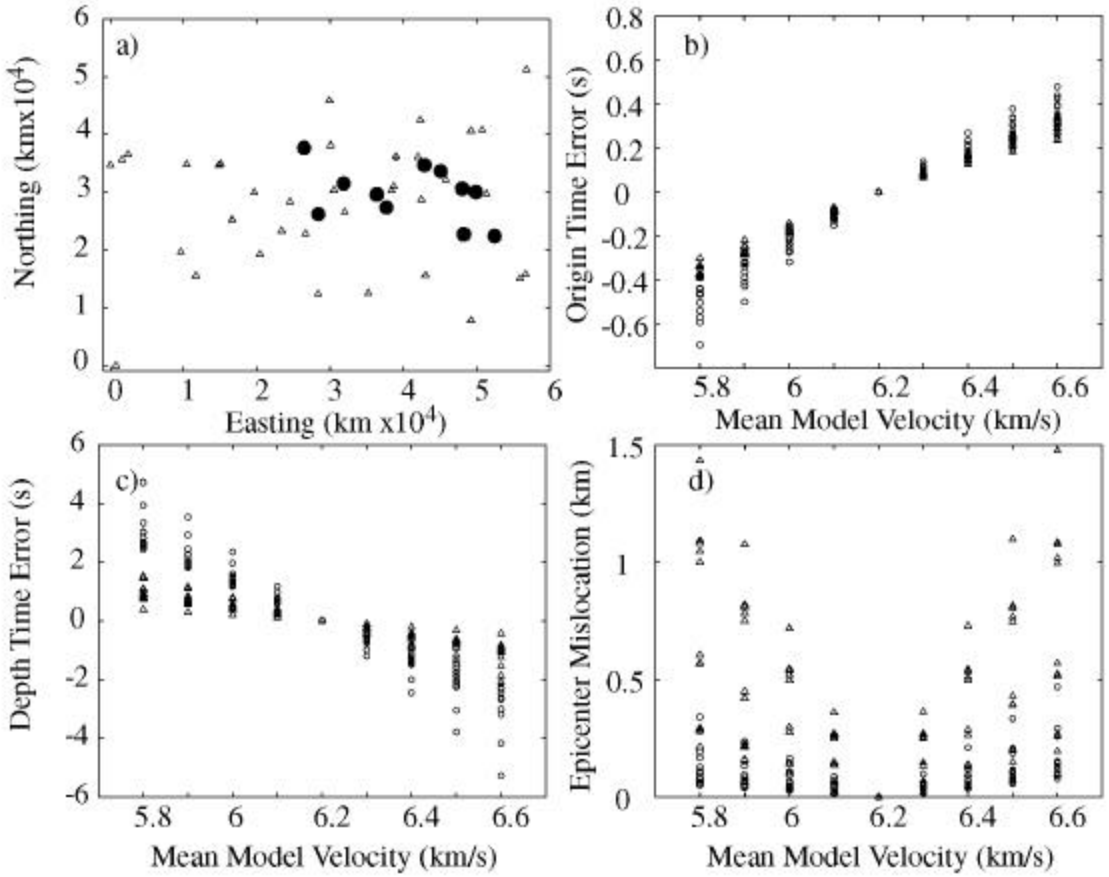
a)
Northing (kmx10^4)
Easting (km x10^4)
b)
Origin Time Error (s)
Mean Model Velocity (km/s)
c)
Depth Time Error (s)
Mean Model Velocity (km/s)
d)
Epicenter Mislocation (km)
Mean Model Velocity (km/s)

Fig. 13

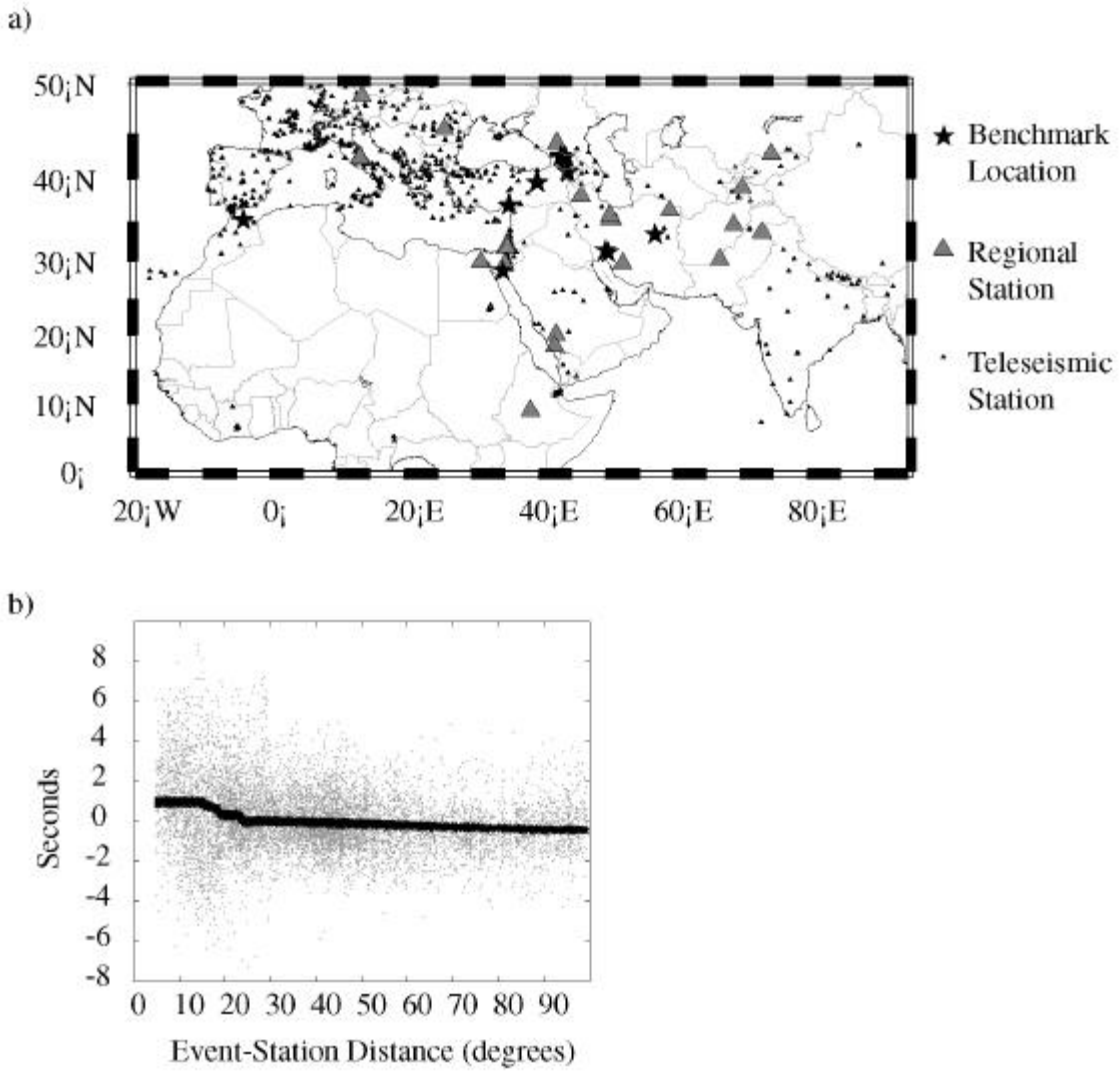
a)
50¡N
40¡N
30¡N
20¡N
10¡N
0¡
20¡W
0¡
20¡E
40¡E
60¡E
80¡E
Benchmark Location
Regional Station
Teleseismic Station
b)
Seconds
8
6
4
2
0
-2
-4
-6
-8
0 10 20 30 40 50 60 70 80 90
Event-Station Distance (degrees)

Fig. 14